Fate of polystyrene and polyethylene nanoplastics exposed to UV in water

Gireeshkumar Balakrishnan, Fabienne Lagarde, Christophe Chassenieux, Arnaud Martel, Elise Deniau, Taco Nicolai

Fate of polystyrene and polyethylene nanoplastics exposed to UV in water

Gireeshkumar Balakrishnan*, Fabienne Lagarde, Christophe Chassenieux, Arnaud Martel, Elise Deniau, Taco Nicolai

IMMM UMR-CNRS6283, Le Mans Université, 72085 Le Mans Cedex 9, France.

*Corresponding author: Dr. Gireeshkumar Balakrishnan

Postal address : IMMM UMR-CNRS6283, Le Mans Université, 72085 Le Mans Cedex 9, France.

Email address: Gireeshkumar.Balakrishnan_Nair@univ-lemans.fr

Abstract

The possible presence of plastic particles with a size smaller than 1 µm in the aquatic environment raises widespread concern over their environmental impact. Therefore, it is important to understand whether and to what extent nanoplastics dispersed in water degrade under UV irradiation. To address this issue, we studied the effect of UV irradiation on monodisperse polystyrene (PS) latex particles with hydrodynamic radii 0.10, 0.25, 0.52, and 2.5 µm as well as on polydisperse polyethylene (PE) particles with an average hydrodynamic radius of 0.35 µm. The degradation rate of both polymers was studied under high intensity UV irradiation, while only the degradation of PS was studied under simulated sunlight, as the degradation of PE was too slow in this case. The degradation was characterized with light scattering techniques, confocal laser scanning microscopy, UV visible spectroscopy, and total organic carbon (TOC) analysis. All particles were found to fully degrade, but the degradation rate of PS particles was much faster than that of PE particles. Aggregation of PS particles

after the addition of sea salt did not inhibit their degradation under UV irradiation. TOC analysis showed that the large majority of the carbon of the polystyrene was converted into volatile products. Interestingly, both polymers, PS and PE, showed no change in the radius of the particles until their mass had decreased by more than 70%, implying that degradation mainly occurred within the particles through the release of organic molecules. The formation of hollow particles and their final fragmentation were confirmed by CLSM microscopy. It was estimated that complete degradation of nanoplastics dispersed in water and exposed to simulated sunlight takes about a month for PS and 2 years for PE, assuming that the effect of the radiation intensity was the same for PE as was determined for PS.

KEYWORDS. Nanoplastics, microplastics, nanoparticles, UV irradiation-induced degradation, polyethylene, polystyrene

1. Introduction

There is growing concern over plastic waste in the marine environment. In the last 50 years, huge quantities of plastics entered the aquatic environment where they have been accumulating with unknown lifetimes [1, 2]. Once in the marine environment, plastics undergo transformation, weathering and degradation and with possible fragmentation and/or erosion leading to the formation of microplastics and nanoplastics. Microplastics constitute a huge family of particles with sizes up to 5 mm displaying various shapes and chemical natures making it difficult to characterize their impact on marine life [3, 4]. Secondary nanoplastics with a size smaller than 1 µm can be released from macro and microplastics by strong mechanical abrasion of plastics such as milling [5] or rotational abrasion [6], but may also be the result of weathering [3,7, 8, 19, 9-11.] In addition, primary micro- and nanoplastics are used in a range of industrial products and may be unintentionally released into the environment [12]. Ter Halle et

al [13] reported for the first time their presence in the North Atlantic Gyre. Since then, nanoplastics have also become an increasing concern as their impact on organisms might be very important [14, 15].

Whereas, the breakdown of macroplastics into micro and nanoplastics under environmentally relevant conditions has been investigated extensively in the last years [3, 8,7, 19, 9-11, 16], relatively few studies have reported on the ultimate fate of nanoplastics in the aquatic environment under UV-irradiation [17]. Concerning microplastics, very recently, Liu et al. [18] reported a study of the degradation of polystyrene (PS) microparticles suspended in water during high intensity UV-irradiation in which they measured the size and number of the resulting particles. They observed that initially cavities were formed within the particles that subsequently break-up into smaller ones [18] with the production of large amounts of nano/microsize fragments. Zhu et al [19] studied the degradation of several types of microplastics under sunlight and they showed that dissolved organic carbon (DOC) was the major by-product of sunlight-driven plastic photodegradation. Similarly, Ward et al [20] showed that the complete oxidation of PS particles could occur within decades, producing CO_2 and dissolved organic carbon as the main products. Considering that nanoplastics are smaller than microplastics, it could be expected that their conversion into dissolved organic carbon should be quite fast. However, Paik et al [21] reported that the lifetime of thermodegraded polypropylene nanoparticles was moderately high compared to the polypropylene microparticles and other studies suggested that fragmentation process could be limited at small scales [22]. Understanding the fate of nanoplastics is very important in view of their persistence and accumulation and their possible release of toxic plastic leachates and degradation products.

Therefore, the objective of the present study was to understand the fate of nanoplastics suspended in water under the influence of UV irradiation. Aqueous suspensions of

commercial monodisperse PS latex particles with different well-defined sizes and polydisperse PE nanoparticles that were prepared as described elsewhere [23], were irradiated using a high intensity UV lamp. Complete degradation under simulated sunlight could be studied for PS particles, but was too slow to achieve for PE particles. The molar mass and hydrodynamic radius were measured as a function of the irradiation time using static and dynamic light scattering techniques. As far as we know, this is the first investigation where both static and dynamic light scattering techniques were combined to understand the photo-degradation mechanism of nanoplastics in water. We will show that measuring both the molar mass and the hydrodynamic radius during the degradation process is needed to fully describe the degradation mechanism. Moreover, the total organic carbon in the aqueous phase was monitored and allowed us to show the formation of volatile breakdown products.

PS is a major pollutant, but we are aware that understanding the degradation of PE is more relevant as it is far more common in the environment. Nevertheless, in this study PS particles were studied in more detail than PE particles, because they are commercially available in many well-defined sizes and degrade much faster. PS particle suspensions are therefore excellent model systems to study the effect of size on the degradation mechanisms and speed. The comparison of light scattering measurements on PS and PE particles during irradiation showed that the degradation process on the colloidal length scale is similar even though it occurs at different rates. As indicated above, PE degradation was found to be too slow under simulated solar irradiation for the study to be feasible. However, we were able to obtain realistic estimates of the degradation rate of PE nanoparticles in the natural environment by assuming that the effect of high-intensity UV irradiation and simulated solar irradiation on the degradation rate of PS nanoparticles was approximately the same for PE particles. To the best of our knowledge, this is the first study in which both the change of

molar mass, size and structure of the small micro- and nanoplastics and the release of volatile organic carbon were monitored during photodegradation.

2. MATERIALS AND METHODS

2.1. Materials

Model polystyrene latex particles with 4 different hydrodynamic radii (R_{hz}) varying by more than one order of magnitude (R_{hz} =0.10, 0.25, 0.52 and 2.5 μm) were purchased from Polysciences. According to the provider, the particles were negatively charged due to the presence of carboxylate groups on their surface which make them stable against aggregation. The 2.5 μm particles contain some divinylbenzene as the cross-linker. However, all other particles are free of any additives. The density of the polystyrene particles was 1.05 g/cm^3.

Polyethylene particles were prepared without any surfactant using an emulsions of toluene in water with PE dissolved in the toluene phase as described in reference [23]. The toluene and water were removed by freeze-drying the emulsion which yields PE particles with R_{hz} ranging between 0.2 to 0.8 μm. After freeze-drying, the PE powder was free of toluene which was confirmed with Raman spectroscopy and thermogravimetric analysis. It was shown that a small amount of PE particles could be dispersed in ultra-pure water without adding a surfactant forming a stable dilute suspension. It was speculated that the stability was in this case due to accumulation of charges onto the particles. The suspension of PE particles was filtered through 1 μm pore size filters. Light scattering measurements showed that after filtration, the R_{hz} of the PE particles ranged between 0.1-0.5 μm with an z-average R_{hz} = 0.35 μm.

2.2. Light scattering

Static and dynamic light scattering measurements were done using commercial equipment ALV/CGS3 (ALV-Langen, Germany) and quartz cells containing either PS or PE particles in ultrapure water. We verified that at the low concentration (5 mg/L) at which these

measurements were done the effect of interaction between the particles was negligible. The light source was a He-Ne laser with wavelength $\lambda = 632$ nm. The temperature was controlled by a thermostat bath at 20 ± 0.2 °C. Measurements were made at angles of observation (θ) between 13 and 150 degrees which correspond to a scattering vector (q) range between 3×10^6 and 3×10^7 m^{-1}. We have used toluene as the standard.

In a static light scattering experiment, the time-averaged scattering intensity of the sample (suspended particles and solvent) was measured as a function of θ. The relative intensity of the suspended particles, Irel, was then calculated by subtracting the intensity of the solvent and dividing by that of a standard, for which we used toluene. I_{rel} is related to the weight average molar mass (M_w) and the structure facture (S(q)) [24-26] of the particles according to:

$$I_{rel}=KCM_w S(q) \quad (1)$$

where K is an optical constant that depends on the setup and the specific refractive index increment of the solute. S(q) describes the dependence of the scattered intensity on the scattering vector q and for particles of any shape, the initial q-dependence of S(q) can be expressed as a series expansion in terms of the z-average radius of gyration (R_g).

$$S(q) = \left[1 + \frac{q^2 {R_g}^2}{3} + ..\right]^{-1} \quad (2)$$

In dilute solution, S(q) depends on the shape of the particles and is equal to 1 for $q\rightarrow0$. In order to measure the molar mass of particles with light scattering the condition $q.R << 1$ must be met. This cannot be done for particles with R = 2.5 µm where we can detect no plateau values for I_{rel} at the lowest investigated q values by opposition to what is shown in fig. 1 and fig. S6.

In a dynamic light scattering experiment, fluctuations in the scattering intensity around the time-averaged value discussed above are measured to obtain the diffusion coefficient (D) and the z-average hydrodynamic radius (Rhz) of the particles. First, the autocorrelation functions of the intensity $g_2(t)$ are measured for different values of θ. Then, the autocorrelation functions of the electric field ($g_1(t)$) are derived from $g_2(t)$ using the Siegert relation [24-26]. In this work, $g_1(t)$ was fitted with a monomodal relaxation time distribution (A(τ)) according to :

$$g_1(t) = \int A(\tau) \exp\left(\frac{-t}{\tau}\right) d\tau \quad (3)$$

with

$$A(\tau) = H\tau^p \exp\left(-\frac{\tau}{\tau_{gex}}\right)^s \quad (4)$$

where H is a normalization constant, τ_{gex} is a characteristic relaxation time and p and s are parameters that characterized the different shape of the distribution. In dilute solutions the relaxation time is related to the diffusion coefficient of the particles:

$$\tau = 1/(Dq^2) \quad (5)$$

R_{hz} can be calculated from D using the Stokes-Einstein relation.

$$D = \frac{kT}{6\pi\eta R_{hz}} \quad (6)$$

where k is the Boltzman constant, T is the absolute temperature and η the viscosity of the solvent. In this manner A(τ), the relaxation time distribution obtained at $q \rightarrow 0$ can be transformed into a distribution of R_{hz}. The z-average hydrodynamic radius (R_{hz}) was calculated from the average diffusion coefficient obtained at $q \rightarrow 0$.

2.3. Confocal laser scanning microscopy (CLSM)

Morphological changes of PS particles in suspension were investigated utilizing a Zeiss LSM 800 (Oberkochem, Germany). A water immersion objective lens was used (HCxPL APO 63× NA = 1.2) with a theoretical resolution of 0.1 μm in the x–y plane. The PS particles were fluorescently labelled by adding Nile red or Fluorescein isothiocyanate (FITC) that spontaneously adsorbed to the particles. The stock solutions of Nile red and FITC were prepared in ethanol and in water, respectively. The concentration of the fluorophore was 5 ppm in the particle suspension. FITC or Nile red was added after the UV irradiation because they bleach during irradiation. Initially, all the Nile red was bound to the PS particles. At longer irradiation times when most of the PS had degraded we observed the formation of dense and bright crystals of Nile red, which, however, could be easily distinguished from the PS particles. At longer UV irradiation time, we also used FITC to confirm the observations obtained with Nile red.

2.4. UV-visible spectroscopy

The UV-visible spectrum of PS particle suspensions at the different ageing times was recorded with a UV–visible spectrometer (Jasco PAC-743). The absorbance (A) was recorded between wavelengths 200-900 nm with a scan speed of 400 nm/minute at a temperature of 20°C. The path length of the light through the cell was 1 cm. With this setup, absorbance measurements are reliable up to 4.

2.5. Total organic carbon analysis (TOC)

TOC analysis was performed on PS latex particles with R_{hz} = 2.5 and 0.25 μm and the samples (C = 100 mg/L) at different irradiation times were diluted by a factor of 4 before performing TOC measurements. The analysis was done, using a Multi N/C 3100 (Analytik Jena) TOC analyzer equipped with an autosampler. The TOC values are measured based on

the integration signals of CO_2 by the infrared detector for total carbon (TC) and total inorganic carbon (TIC). The TOC value is calculated as TOC = TC-TIC. The vials used as containers for the TOC analyses were kept in an oven at 500°C for 8h to avoid any trace of organic matter and cooled down before further use. The conditions used in the method were as follows: from 5 to 8 measurements were performed with a coefficient of variation below 2%. The sample volume was 200 µL and the rinse volume was 1 mL. The integration time was 300 s and the stirring rate was fixed to 6. For TC measurements, the combustion temperature was set to 750°C. IC measurements were performed in the IC reactor with H_3PO_4 10% wt. For TIC, three calibrations were performed between 0.1 and 100.0 mg/L corresponding to a limit of detection based on the lowest calibration curve equal to 33.7 µg/L. For TC, three calibrations were also performed ranging from 1.0 up to 1000.0 mg/L leading to a limit of detection based on the lowest calibration curve of 112.1 µg/L. The average of three values differing by less than 2% was taken. We note that the measured values were always three times bigger than the detection limit and remained within the calibration range.

2.6. Irradiation

Two kinds of set-ups were used to UV irradiate the PE and PS suspensions. In order to simulate sunlight exposure, the samples were placed in a commercial solar exposure simulator (XLS+ chamber, Atlas), which is equipped with a xenon lamp, see figure S1a. Weathering was achieved with a daylight filter following the ISO 4892-2 standard at 40°C and a black standard temperature of 65°C. The irradiation intensity was 60 W/m², which corresponds to a solar radiation exposure of 216 $kJ.m^2.h^{-1}$. To accelerate the process further, the suspensions were also irradiated using a high intensity UV lamp. The high intensity UV lamp (HTC 400-241 SUPRATEC HTC/HTT, OSRAM GmbH) was used without any filter and was fixed inside a black box at a distance of 75 cm from the irradiated samples, see figure S1b of the

supplementary information. The same lamp has been used earlier for the accelerated weathering of plastics [27]. The temperature inside the quartz tubes was between 40 and 50°C due to the heat from the UV lamp. The intensity of the lamp near the sample was around 360 W/m², i.e. 6 times higher than with the solar chamber. We note that the spectra of the two UV light sources are not the same, see figure S2

For the analysis by light scattering techniques, PE or PS particle suspensions at C = 5 mg/L in ultrapure water (Millipore) were placed in capped quartz cells with an inner diameter of 8 mm. The tubes were placed at an angle so that the total path length of the light through the sample was 10 mm. These samples were transparent and the intensity of UV light was almost the same over the whole depth. The samples were regularly homogenized during irradiation and before the light scattering measurements by handshaking.

For TOC, CLSM, and UV-visible spectroscopy measurements on PS particles with radii of 2.5 µm and 0.25 µm, a quartz beaker containing 80 ml of the PS suspension at C=100 mg/L was placed under the high intensity UV lamp, while gently stirring with a magnetic stirrer to avoid sedimentation and ensure uninform UV exposure. 10 ml of the suspension was removed from the beaker at regular time intervals during the UV irradiation for the TOC analysis. During irradiation, the beaker was closed with a quartz cap and the sides of the cap were sealed with Teflon tape to avoid evaporation. These samples were only weakly turbid, which means that the UV-irradiation was on average less intense than for the dilute samples used for light scattering analysis. Therefore, ageing is expected to be somewhat slower. However, this effect became progressively less important as more of the sample was removed so that the path length through the sample decreased from the initial 80 mm. A scheme of the experimental set-up is shown in figure S3.

Two different initial concentrations (c=5 mg/L and C=100 mg/L) of PS particles because for light scattering experiments the sample need to be transparent and therefore

diluted whereas visually the breakdown is more easily seen at high concentration. It also allowed us to study the effect of concentration in terms of the penetration of the UV light in more turbid samples.

The reproducibility of the treatment was tested by irradiating at least two independent samples of the same systems. The results were combined in figs 3 and 5, which showed that the reproducibility is very good.

3. Results and Discussion

3.1. Degradation of PS particles during high intensity UV irradiation

The degradation of the PS particles with initial hydrodynamic radii R_{hz} = 0.10, 0.25 and 0.52 µm was quantified by measuring their molar mass and radius after different UV irradiation times by light scattering techniques. Reliable light scattering measurements require that the suspension is transparent. Therefore, we did these measurements at a low concentration of PS particles (C = 5 mg/L), at which the suspensions were transparent and interaction between the particles was negligible. This means that all particles received the same irradiation. For comparison, the behaviour of the particle suspensions was also studied as a function of time in the dark. Figure S4 of the supplementary information shows the q-dependence of the scattering intensity for samples kept at different times in the dark. It is characteristic for monodisperse spherical particles and no change was observed even after 120 hours indicating that the particles did not degrade when not irradiated. No aggregation upon time was detected either. Note that even weak aggregation is easily detected by light scattering as the scattered light intensity is proportional to the molar mass, see eq. 1.

Figure 1 displays the results that have been obtained for the PS particles with R_{hz} = 0.10 µm and 0.25 µm after different UV irradiation times. A systematic decrease of the relative intensity (I_{rel}) was observed with increasing UV irradiation which means that the

molar mass of the particles decreased assuming that their refractive index increment, and thus K, does not change significantly, see eq. 1. Interestingly, up to 48 h irradiation no significant change of the q-dependence was observed, which means that the form and size of the particles remained unchanged. After 72 h irradiation, particles could still be detected. However, the q-dependence of I_{rel} showed that the particles were no longer spherical and monodisperse. After 96 h, the scattering intensity was not significantly higher than that of Millipore water, see figure S5 of the supplementary information, and no particles were detected, which shows that the particles had fully degraded. Similar results were obtained for particles with R_{hz} = 0.52 µm as shown in figure S6 of the supplementary information.

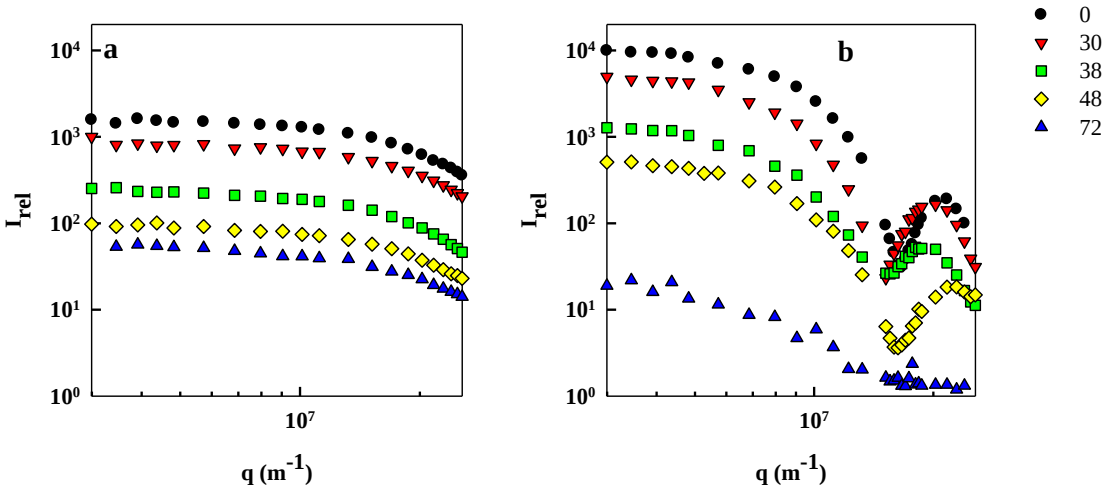

Figure 1. Double logarithmic plot of the relative scattering intensity as a function of q for PS particles in ultrapure water with initial R_{hz} = 0.10 µm (a) and 0.25 µm (b) at different high intensity UV irradiation times in hours as indicated in the legend which is the same for both figures.

The relative decrease of $I_{rel}(t)$ at $q \rightarrow 0$ with respect to the initial value is plotted in Figure 2a as a function of irradiation time showing a sharp decrease after 24 h whatever the size of the pristine particles. I_{rel} at $q \rightarrow 0$ is proportional to $C.M_w$ if we assume that the specific

refractive index increment of the particles does not change significantly upon irradiation, see eq.1. It seems furthermore reasonable to assume that all particles degrade at approximately the same rate so that the molar concentration of particles ($\nu=C/M_w$) does not decrease during irradiation. It follows that I_{rel} at $q\rightarrow 0$ is proportional to M_w^2 and that the decrease of I_{rel} implies a decrease in the molar mass of the particles. The relative decrease was the same for all PS particles, but at longer times ($T \geq 30$ h) the particles with R_{hz} = 0.52 µm degraded more rapidly. The time needed to decrease by half the amount of PS in the particles can be estimated from the decrease of the molar mass and was approximately 30 hours for R_{hz} = 0.52 µm and 34 hours for the smaller particles. The decrease of the molar mass was observed to start after some lag-time, which suggests that the removal of material from the particles was preceded by chemical modifications that need to progress up to a certain point before material can escape. Notice that figure 2 contains results obtained from independent measurements on different samples of particles with the same size, showing good reproducibility of the breakdown process.

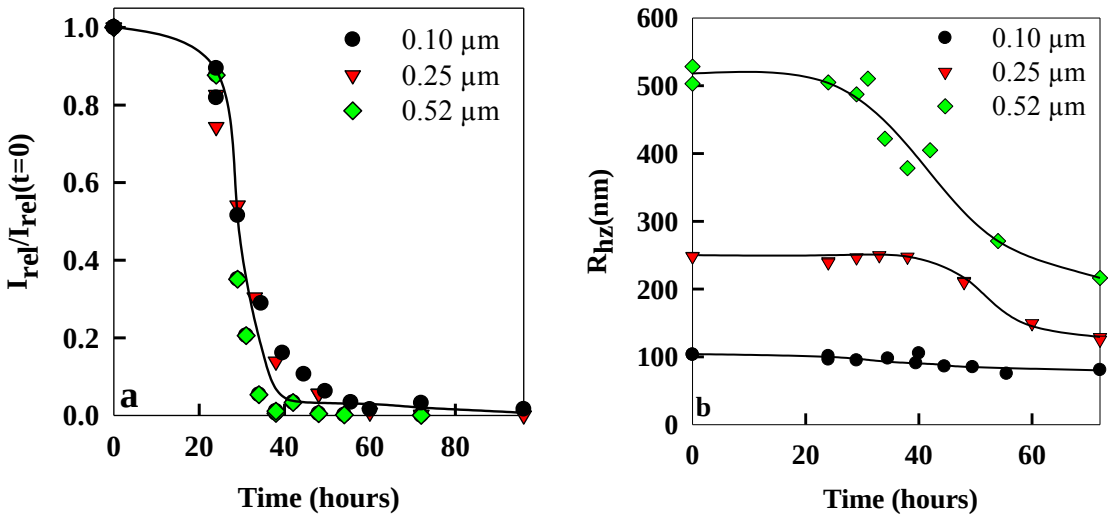

Figure 2. (a) I_{rel} with respect to the initial value as a function of high intensity UV irradiation time for suspensions of PS particles at C=5 mg/L with three initial radii as indicated in the

figure. (b) The average hydrodynamic radius of PS particles with three different initial radii as a function of the irradiation time.

Analysis of the autocorrelation functions determined with DLS on the same samples showed narrow relaxation time distributions from which R_{hz} could be determined, as described in section 2.2. The dependence of R_{hz} on the irradiation time is shown in Figure 2b. R_{hz} remained the same up to 40 h for particles with initial R_{hz} = 0.10 and 0.25 µm and decreased weakly at longer times. The size of particles with initial R_{hz} = 0.52 µm had already decreased significantly after 40 hours of UV irradiation. Interestingly, when comparing fig 2a and b, it appears that the degradation of the particles induced by UV-radiation did not cause a change in their size until their mass had decreased very substantially. The implication is that the material was not preferentially removed from the surface, but rather from the interior of the particles. This degradation phenomenon was induced by UV radiation, as no degradation was observed for particles kept in the dark, see figure S4. UV light can easily penetrate relatively small particles, which explains why degradation occurred everywhere and not specifically on the surface.

We also investigated the effect of the initial concentration of PS particles with R_{hz} = 0.25 µm by increasing the concentration from 5 to 100 mg/L. At C = 100 mg/L the suspension was initially turbid, see figure 3. The suspension was irradiated at different UV irradiation times under gentle stirring to avoid uneven exposure to UV. Figure 3 shows the evolution of the visual appearance of a PS particle suspension at different UV irradiation times. The turbidity of the particle suspension decreased with increasing UV irradiation and after 72 hours it became transparent. M_w and R_{hz} of the PS particles at different UV irradiation times were determined after dilution to C = 5 mg/L. In Figure S7(a) we compare the relative

decrease of $I_{rel}(t)$ at $q \rightarrow 0$ with respect to the initial value as a function of the irradiation time for particles aged at C=5 mg/L and aged at C=100 mg/L. The corresponding comparison for R_{hz} is shown in figure S7(b). As expected, the degradation rate was slower for the turbid suspensions due to the lower average irradiation intensity received by the particles. However, in both cases the degradation mechanism was the same, i.e. material was preferentially removed from within the particles.

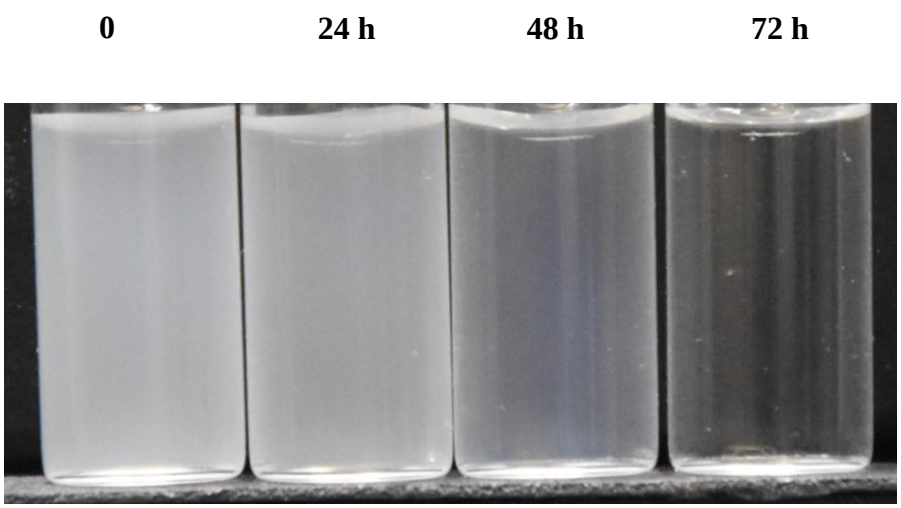

Figure 3. Effect of high intensity UV irradiation time on the turbidity of a suspension of PS particles with R_{hz} = 0.25 µm at C = 100 mg/L. The particle suspension was stirred gently during irradiation.

In order to observe the morphological changes during UV irradiation with CLSM we studied a suspension of larger PS particles with R_h = 2.5 µm at C=100 mg/L. The particles were stirred gently during irradiation. After the UV irradiation, the particles were labelled with Nile red. We note that no fluorescence was detected without adding a fluorophore. Figure 4 shows images of the PS particle suspensions at different ageing times. Up to 40

hours of irradiation the fluorophore rapidly distributed homogeneously throughout the particles. However, after 60 h irradiation, the fluorescence was no longer homogenously distributed within the particles but appeared to be localized, which suggests the removal of material from the interior of the particles. After 72 h most particles showed a strong fluorescent shell with almost no fluorescence from the inside. After 96 h UV irradiation, smaller particles were formed, probably due to the break-up of larger ones. Finally, no particles were detected after 120 h of UV irradiation. It is clear that all particles were broken down at approximately the same rate, which justifies the assumption that the decrease of the scattering intensity corresponds to a decrease of the molar mass of the particles. These results are in agreement with those reported by Liu et al [18]. mentioned in the Introduction.

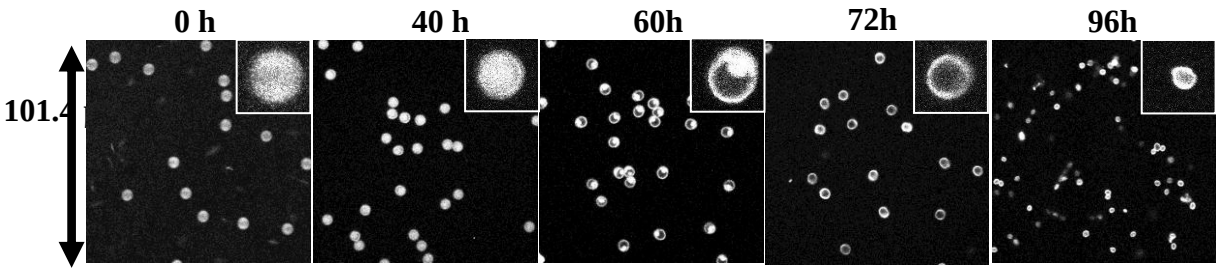

Figure 4 CLSM images of a PS particle suspension (R_{hz} = 2.5 µm) at high intensity UV irradiation times as indicated in the figure. Images of individual particles at higher magnification (7.5 µm x 7.5 µm) are shown in the insets. The particle suspension at C = 100 mg/L was stirred gently during irradiation.

The results from light scattering and confocal microscopy are in agreement and show that the degradation of PS particles upon irradiation was not restricted to their surface. Material was mostly removed from the interior of the particles, which explains why the breakdown occurred at approximately the same rate for particles of different sizes, see figure 2a. Here we used spherical particles, whereas nanoplastics formed by weathering or abrasion are not expected to be spherical. However, since the material is mostly removed from the

interior of the particles, we don't expect the shape to play a major role in the degradation rate as long as the UV-light can penetrate to the core of the particles. However, if the particles are so large that a significant fraction of the UV light cannot penetrate them, the shape of the particles will become an important parameter to take into account.

When the particles sediment or cream and form a thick dense layer, the UV light cannot penetrate all particles. This is what happened when PS particles with R_{hz} = 2.5 µm at C=100 mg/L, were exposed to UV without stirring, leading to the formation of a thick particle layer at the bottom of the quartz beaker due to sedimentation. It explains why we found that the degradation rate of sedimented particles was slower than when sedimentation was avoided by stirring, see figure S8 and figure S9 of the supplementary information for CLSM images of the particles labelled with Nile red and FITC, respectively. We noticed that FITC adsorbed to the particles only after more than 24 h UV irradiation. The reason is most likely that UV irradiation chemically modified the particles. From figure S8 and figure S9 it is clear that without stirring, only a few particles were degraded from the inside at t = 72 h, but most of the particles were affected between t = 96 and 120 h. After 178 h UV irradiation, smaller particles were also formed. No particles were detected by confocal microscopy after 216 hours of UV irradiation. This indicates that the degradation rate was slower without stirring, but in both cases, degradation started from the inside.

Figure 5 shows the absorbance spectra of PS particles with R_{hz}=0.25 µm at C= 100 mg/L after different durations of irradiation while stirring gently. The spectra are in agreement with the UV visible spectrum of polystyrene earlier reported in the literature [20, 28]. Before irradiation, the spectrum showed an absorbance peak at 250 nm together with the effect of turbidity that decreased with increasing wavelengths. The absorbance peak at 250 is due to the aromatic ring of the polystyrene as was reported elsewhere [20, 28]. After 24 h irradiation, the turbidity of the suspension had decreased, but the amplitude of the absorbance

388 at 250 nm showed a weak increase. However, after 48 h irradiation, the absorbance peak at
389 250 nm had completely disappeared and was replaced by a strong increase of the absorbance
390 at lower wavelengths, whereas the effect of the turbidity continued to decrease. At longer
391 times the absorbance at low wavelengths decreased also and after 120 h irradiation, it had
392 become negligible.

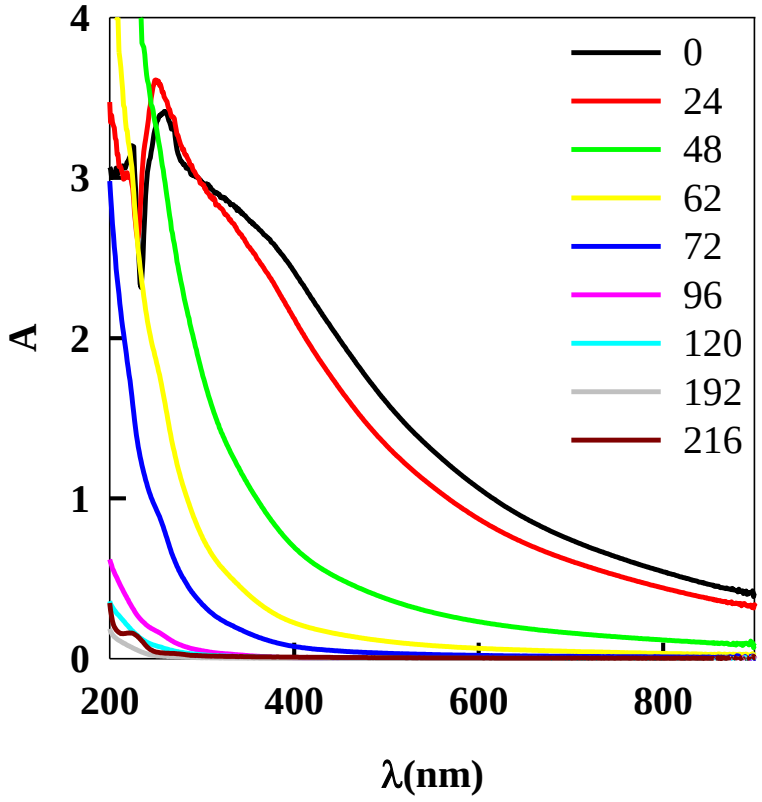

393

394 Figure 5. Absorbance spectra of a suspension of PS particles with R_{hz} = 0.25 µm at 100mg/L
395 as a function of high intensity UV irradiation time as indicated in the graph.

396 The disappearance of the peak at 250 nm suggests that PS was chemically modified
397 within the first 48 h and that breakdown products were formed that strongly absorbed UV
398 light at lower wavelengths. These products were subsequently degraded by further irradiation.
399 Similar results were obtained for PS particles with R_{hz} = 2.5 µm at C= 100 mg/L during
400 irradiation while gently stirring, see figure S10 of the supplementary information. Here a

401 strong increase in the absorbance appeared at lower wavelengths that disappeared after longer
402 irradiation times. However, these larger PS particles showed a broad absorbance peak centred
403 at 650 nm of which we do not know the origin. This peak also disappeared during irradiation
404 and after 120 h the absorbance had become negligible.

405 It has been reported that photodegradation of PS leads to the formation of short
406 polymer chains or other small molecules [27, 29-32] or even carbon dioxide [20]. Here we
407 investigated the total organic carbon content (TOC) of the suspensions of PS particles with R_h
408 = 2.5 and 0.25 µm at different irradiation times, see figure 6. A weak decrease of the TOC
409 was observed until approximately 40 h irradiation followed by a strong decrease. The rate of
410 decrease of the TOC was independent of particle radius up to 120 h of irradiation in
411 agreement with the light scattering results shown above. The decrease shows that PS was
412 broken down into volatile molecules, probably carbon dioxide [20]. After 219 h irradiation, the
413 TOC in the solution was reduced from 30 mg/L to 2.5 and 6 mg/L for the particles with R_{hz} =
414 2.5 and 0.25 µm, respectively, see figure 6.

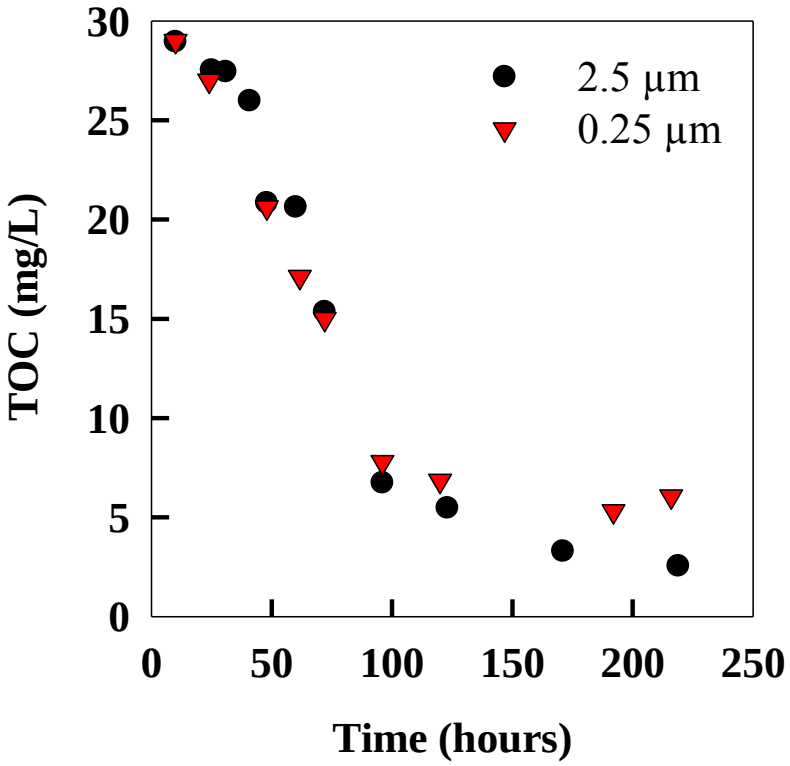

Figure 6. The decrease of total organic carbon content for a suspension of PS particles with R_{hz} = 2.5 and 0.25 µm as a function of high intensity UV irradiation time.

At a given UV irradiation time, the TOC consists of both colloidal PS particles and dissolved carbon formed during degradation. The amount of dissolved carbon can be estimated for particles with R_{hz} =0.25 µm by comparing light scattering measurements and TOC measurements, because the relative decrease of the molar mass of the particles is equal to the relative increase of the sum of the dissolved and volatilized carbon. In figure 7 the relative decrease of molar mass was computed from the square root of the relative decrease of the scattering intensity displayed in figure S7 a. Figure 7 shows that the molar mass decreased faster than the TOC, which means that the carbon from the PS was first converted into soluble carbon and subsequently into volatile carbon in agreement with the evolution of the UV

spectra. About 20% of the carbon did not volatilize even after very long irradiation times when all the PS particles had long since completely degraded.

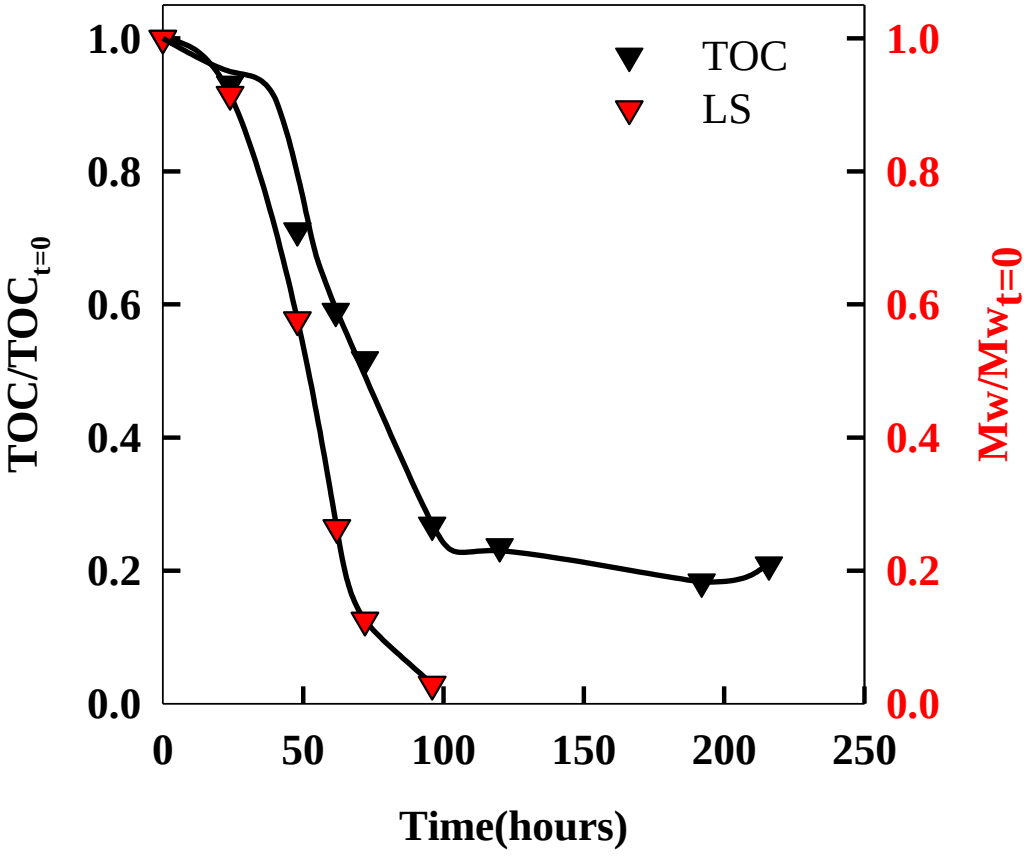

Figure 7. Comparison of the relative decrease of the TOC and M_w with time under high intensity UV irradiation for particles with R_{hz} = 0.25 µm, the particle suspension was aged at C=100 mg/L.

As mentioned in the introduction, Ward et al [20] showed that photodegradation of PS leads to complete degradation into CO_2 for samples with a thickness below 200 µm. The authors estimated that in natural sunlight this process takes a few decades assuming that CO_2 production increases linearly with UV irradiation times. However, here we observed that in the case of PS the rate of mass loss during UV irradiation is not linear with time but

accelerates after some time, see figure 2a. This implies that the time required for the complete degradation of PS in the natural sunlight is much shorter than that estimated by Ward et al [20].

3.2. Degradation of PS particles in simulated sea water

The stability of nanoplastics in the sea may be different from that in salt-free water. Therefore, we studied the degradation of PS particles with R_{hz}= 0.25 µm in simulated seawater produced by adding 35 g/L sea salt to Millipore water, i.e. approximately the same concentration as in natural seawater. Weak aggregation of the particles occurred as soon as the salt was added to the particle suspension, caused by the screening of electrostatic repulsion between the particles by the salt. During the first 24 h of UV irradiation, the aggregates grew in size and became visible to the eye, but subsequently, they disappeared gradually with increasing irradiation time, see figure S11. A transparent solution was formed after 168 h irradiation. UV induced aggregation of nanoplastics in salty water was reported by various authors[33-36] but their complete degradation has been rarely discussed in the literature. No significant visual changes were observed in the dark for up to at least 7 days. This observation shows that even if the particles are in the aggregated state, they can be degraded by UV irradiation, albeit at a slower rate.

3.3. Degradation of PS particles during simulated solar irradiation

Figure S12 of the supplementary information shows the evolution of the q-dependent relative scattering intensity of a suspension of PS particles with initial R_h = 0.25 µm after different times of simulated solar irradiation. Three independent measurements were performed for the same particle suspension and a good reproducibility is observed in all cases. The behaviour was similar to that observed during high intensity irradiation, but much slower. In figure 8 the evolution of I_{rel} at $q \rightarrow 0$ and R_{hz} during simulated solar irradiation is compared

with that during irradiation with a high intensity UV lamp. The comparison shows that the breakdown under simulated solar light was about 12 times slower than during irradiation with a high intensity UV lamp. The difference in degradation rate was larger than the difference in UV intensity (6 times), which can be explained by the different wavelength distribution of the two UV sources, see fig. S2 of the supplementary information. Even though the rate is slower the degradation process appears to be the same with a decrease of the R_{hz} starting only after I_{rel} had already strongly decreased.

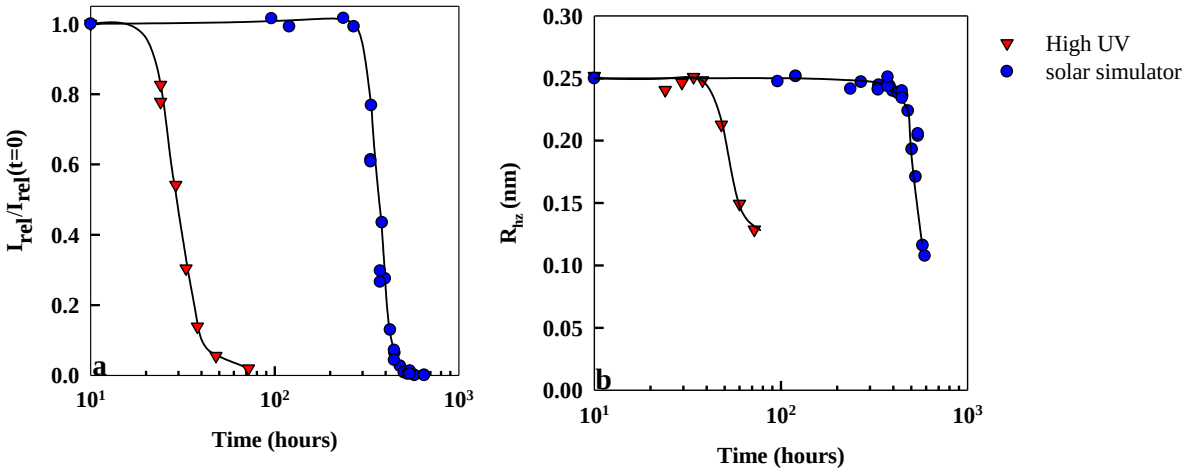

Figure 8. (a) The decrease of I_{rel} with respect to the initial value and of (b) the hydrodynamic radius of PS particles (R=0.25 µm) with UV irradiation time. The blue circle and the red triangle represent data for the aging in the solar simulator and in the high intensity UV lamp, respectively. The legends are the same in Figure 8a and Figure 8b.

3.4. Degradation of PE particles during high intensity UV irradiation

The scattering intensity of PE particles at C = 5 mg/L in the dark and during irradiation with the high intensity UV lamp is plotted in Figure S13a and S13b of the supplementary information, respectively. The suspension of PE particles was observed to be stable in the dark for at least one month. No creaming was observed despite the density of the

PE particles, which can be explained by the low creaming speed given the size of the particles (approximately 0.003 μm/s for a radius of 0.35 μm and a density of 0.9 g/ml). However, during irradiation, a systematic decrease in Irel was observed. In figure 9a the dependence of I_{rel} at $q \rightarrow 0$ on the irradiation time is shown. I_{rel} decreased relatively sharply after about 4 days of irradiation by about 60% after which the decrease became more gradual. R_{hz} remained approximately constant for about 25 days after which it decreased weakly, see figure 9b. The crystalline fraction of the PE used in the investigation was 32% [23]. We speculate that the initial fast decay is due to the degradation of PE in the amorphous region whereas the slow decay corresponds to the crystalline PE.

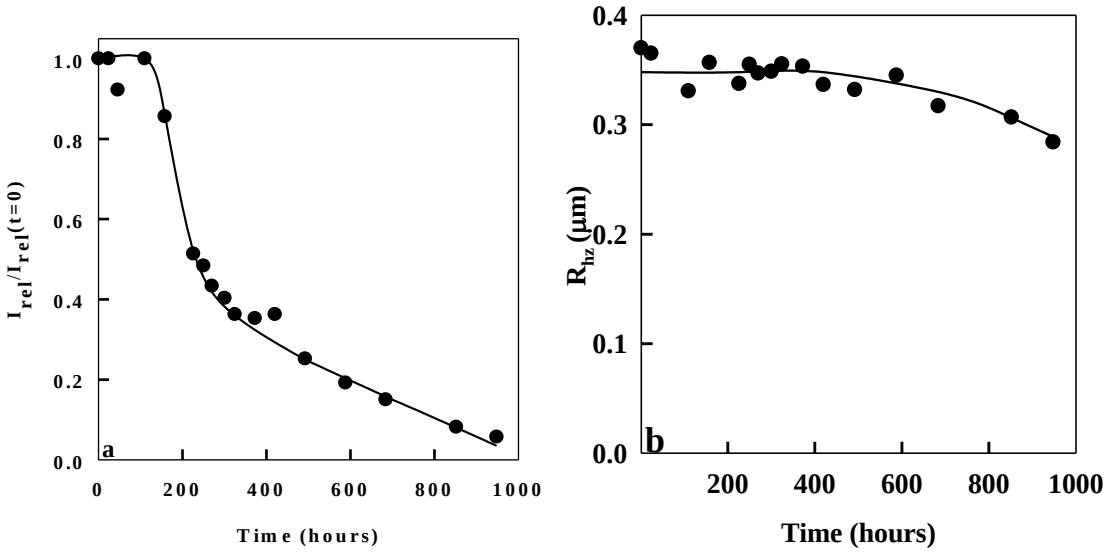

Figure 9. (a)The decrease of I_{rel} with respect to the initial value (b) and the average hydrodynamic radius for a suspension of PE particles during high intensity UV irradiation.

The degradation rate of PE particles was found to be much slower than that of PS particles. The time required to reduce 90% of the relative scattering intensity with a high intensity UV irradiation was around 38 days for PE compared to 2 days for PS particles, see fig. 9a. Considering that $I_{rel} \propto M_w^2$, a 90% reduction of the intensity corresponds to a mass

495 loss of 70%. As for PS particles, the time needed to decrease by half the amount of PE in the
496 particles can be estimated from the decrease of the molar mass and was approximately 20
497 days.

498 Interestingly, a similar degradation behaviour was observed for PE as that of PS, i.e.
499 the M_w of the particles was decreased substantially without changing the radius see figure 2
500 and figure 9. However, the degradation rate was much slower for PE, which implies that the
501 chemical reactions leading to the break-down of PE are very different than for PS. However,
502 for both polymers the break-down is caused by UV radiation, which can easily penetrate both
503 the small PS and PE particles studied, which explains why it is much faster using a high
504 intensity lamp than in simulated sunlight. Therefore, it is reasonable to assume that the effect
505 of the UV source on the degradation rate is approximately the same for PS and PE. For PS
506 particles we found that it was13 times slower under sunlight than under the high intensity UV
507 lamp. Assuming that the degradation rate of PE particles is also 13 times slower under
508 simulated sunlight we find that it will take more than a year to decrease by 70% the molar
509 mass of PE particles suspended in water under simulated solar irradiation.

510 The stronger resistance to UV irradiation of PE compared to PS was also noted in a
511 study by Zhu et al [19]. These authors investigated the photochemical dissolution of buoyant
512 microplastics of PE, PP and expanded PS by monitoring the formation of dissolved organic
513 content (DOC) under natural sunlight exposure. The authors reported that the highest DOC
514 production was for PS followed by PP and then PE. The faster degradation rate of PS is
515 related to its chemical structure which renders it more prone to photo oxidation than
516 polyolefins. Another difference between the PS and PE particles is that the latter was not
517 necessarily spherical. However, given that the degradation rate is independent of the particle
518 size for small particles and starts from the inside, the shape is unlikely to have an influence on
519 the degradation rate except perhaps in the final stage where the particles break-up.

The results reported in the current study show that nanoplastics in aqueous suspension degrade more or less slowly under solar radiation depending on their chemical nature. Degradation does not occur in the dark and therefore requires that the particles are near the surface where the intensity of UV irradiation is still significant. If the particles are larger or aggregate into larger flocs they will sink or float depending on their density. Only when they float they will be subjected to irradiation leading to their degradation. In that case, their rate of degradation is expected to be similar to that found here for small particles as long as the UV light can penetrate them, as was shown here for aggregated PS particles. For instance, at least 50% of UV light penetrates pure PS to a depth of 100 µm [38]. Notice, however, that here we studied pristine PS and PE particles, but in practice, additives that protect against UV or oxygenation can be present. Their presence may lead to a slow-down of the degradation process.

4. Conclusion

Nanoplastics made from polystyrene (R_{hz} = 0.1 – 2.5 µm) and polyethylene (R_{hz} = 0.1 – 0.5 µm) in aqueous suspension fully degrade during irradiation with UV light. Light scattering and CLSM measurements show that initially, mass loss occurs from the interior of the particles rendering the particles increasingly less dense without changing their size. Fragmentation occurs only after the large majority of the mass is lost and the particles have become fragile. The degradation rate was found to be similar for PS particles with radii up to at least 2.5 µm. TOC analysis showed that degradation of PS particles leads to the removal of carbon from the suspension in the form of volatile carbon. The degradation process of PE particles induced by UV irradiation was similar to that of PS particles, but approximately 20

543 times slower than for PS particles. Under simulated sunlight irradiation it takes about one
544 month for PS and 2 years for PE to fully degrade.

545 In more realistic situations it is likely that nanoplastics aggregate. Here we showed for
546 PS particles that the degradation occurs also in the aggregated state. Of course, it is necessary
547 that UV light can penetrate the aggregates, which is easier when they are small and have an
548 open structure. Other issues that will need to be considered in future research are the effect of
549 additives and contaminants that may influence the degradation rate.

550 **Conflicts of interest**

551 There are no conflicts of interest to declare

552 **Acknowledgements**

553 The French National Research Agency (ANR) is acknowledged for the financial support of
554 this project (ANR POEM ANR-21-CE06-0019).

555

References

1. M. A. Browne, T. Galloway and R. Thompson, Microplastic--an emerging contaminant of potential concern?, *Integrated environmental assessment and Management*, 2007, **3**, 559-561.
2. M. Eriksen, L. C. Lebreton, H. S. Carson, M. Thiel, C. J. Moore, J. C. Borerro, F. Galgani, P. G. Ryan and J. Reisser, Plastic pollution in the world's oceans: more than 5 trillion plastic pieces weighing over 250,000 tons afloat at sea, *PloS one*, 2014, **9**, e111913.
3. A. L. Andrady, The plastic in microplastics: A review, *Marine pollution bulletin*, 2017, **119**, 12-22.
4. D. K. Barnes, F. Galgani, R. C. Thompson and M. Barlaz, Accumulation and fragmentation of plastic debris in global environments, *Philosophical transactions of the royal society B: biological sciences*, 2009, **364**, 1985-1998.
5. T. Gardon, I. Paul-Pont, G. Le Moullac, C. Soyez, F. Lagarde and A. Huvet, Cryogrinding and sieving techniques as challenges towards producing controlled size range microplastics for relevant ecotoxicological tests, *Environmental Pollution*, 2022, **315**, 120383.
6. Y. K. Song, S. H. Hong, M. Jang, G. M. Han, S. W. Jung and W. J. Shim, Combined effects of UV exposure duration and mechanical abrasion on microplastic fragmentation by polymer type, *Environmental science & technology*, 2017, **51**, 4368-4376.
7. F. Julienne, N. Delorme and F. Lagarde, From macroplastics to microplastics: Role of water in the fragmentation of polyethylene, *Chemosphere*, 2019, **236**, 124409.
8. S. Lambert and M. Wagner, Characterisation of nanoplastics during the degradation of polystyrene, *Chemosphere*, 2016, **145**, 265-268.
9. N. Meides, T. Menzel, B. Poetzschner, M. G. J. Löder, U. Mansfeld, P. Strohriegl, V. Altstaedt and J. Senker, Reconstructing the Environmental Degradation of Polystyrene by Accelerated Weathering, *Environmental Science & Technology*, 2021, **55**, 7930-7938.
10. T. Menzel, N. Meides, A. Mauel, U. Mansfeld, W. Kretschmer, M. Kuhn, E. M. Herzig, V. Altstädt, P. Strohriegl, J. Senker and H. Ruckdäschel, Degradation of low-density polyethylene to nanoplastic particles by accelerated weathering, *Science of The Total Environment*, 2022, **826**, 154035.
11. J. Qin, S. Zeng, X. Wang, X. Wang and C. Lin, Liberation of plastic nanoparticles and organic compounds from three common plastics in water during weathering under UV radiation-free conditions, *Science of The Total Environment*, 2022, **842**, 156859.
12. A.-K. Müller, J. Brehm, M. Völkl, V. Jérôme, C. Laforsch, R. Freitag and A. Greiner, Disentangling biological effects of primary nanoplastics from dispersion paints' additional compounds, *Ecotoxicology and Environmental Safety*, 2022, **242**, 113877.
13. A. Ter Halle, L. Jeanneau, M. Martignac, E. Jardé, B. Pedrono, L. Brach and J. Gigault, Nanoplastic in the North Atlantic subtropical gyre, *Environmental science & technology*, 2017, **51**, 13689-13697.
14. K. Tallec, A. Huvet, C. Di Poi, C. González-Fernández, C. Lambert, B. Petton, N. Le Goïc, M. Berchel, P. Soudant and I. Paul-Pont, Nanoplastics impaired oyster free living stages, gametes and embryos, *Environmental pollution*, 2018, **242**, 1226-1235.
15. M. R. M. Zaki and A. Z. Aris, An overview of the effects of nanoplastics on marine organisms, *Science of The Total Environment*, 2022, 154757.
16. X. Ren, Y. Han, H. Zhao, Z. Zhang, T.-H. Tsui and Q. Wang, Elucidating the characteristic of leachates released from microplastics under different aging conditions: Perspectives of dissolved organic carbon fingerprints and nano-plastics, *Water Research*, 2023, **233**, 119786.
17. P. Pfohl, M. Wagner, L. Meyer, P. Domercq, A. Praetorius, T. Hüffer, T. Hofmann and W. Wohlleben, Environmental Degradation of Microplastics: How to Measure Fragmentation Rates to Secondary Micro- and Nanoplastic Fragments and Dissociation into Dissolved Organics, *Environmental Science & Technology*, 2022, **56**, 11323-11334.

18. Z. Liu, Y. Zhu, S. Lv, Y. Shi, S. Dong, D. Yan, X. Zhu, R. Peng, A. A. Keller and Y. Huang, Quantifying the dynamics of polystyrene microplastics UV-aging process, *Environmental Science & Technology Letters*, 2021, **9**, 50-56.
19. L. Zhu, S. Zhao, T. B. Bittar, A. Stubbins and D. Li, Photochemical dissolution of buoyant microplastics to dissolved organic carbon: rates and microbial impacts, *Journal of hazardous materials*, 2020, **383**, 121065.
20. C. P. Ward, C. J. Armstrong, A. N. Walsh, J. H. Jackson and C. M. Reddy, Sunlight converts polystyrene to carbon dioxide and dissolved organic carbon, *Environmental science & technology letters*, 2019, **6**, 669-674.
21. P. Paik and K. K. Kar, Kinetics of thermal degradation and estimation of lifetime for polypropylene particles: Effects of particle size, *Polymer degradation and stability*, 2008, **93**, 24-35.
22. C. Brouzet, R. Guiné, M.-J. Dalbe, B. Favier, N. Vandenberghe, E. Villermaux and G. Verhille, Laboratory model for plastic fragmentation in the turbulent ocean, *Physical Review Fluids*, 2021, **6**, 024601.
23. G. Balakrishnan, M. Déniel, T. Nicolai, C. Chassenieux and F. Lagarde, Towards more realistic reference microplastics and nanoplastics: preparation of polyethylene micro/nanoparticles with a biosurfactant, *Environmental Science: Nano*, 2019, **6**, 315-324.
24. B. J. Berne and R. Pecora, *Dynamic light scattering: with applications to chemistry, biology, and physics*, Courier Corporation, 2000.
25. W. Brown, *Dynamic light scattering: the method and some applications*, Clarendon Press, 1993.
26. H. C. Hulst and H. C. van de Hulst, *Light scattering by small particles*, Courier Corporation, 1981.
27. B. Gewert, M. Plassmann, O. Sandblom and M. MacLeod, Identification of chain scission products released to water by plastic exposed to ultraviolet light, *Environmental Science & Technology Letters*, 2018, **5**, 272-276.
28. T. Li, C. Zhou and M. Jiang, UV absorption spectra of polystyrene, *Polymer Bulletin*, 1991, **25**, 211-216.
29. L. P. Domínguez-Jaimes, E. I. Cedillo-González, E. Luévano-Hipólito, J. D. Acuña-Bedoya and J. M. Hernández-López, Degradation of primary nanoplastics by photocatalysis using different anodized TiO2 structures, *Journal of Hazardous Materials*, 2021, **413**, 125452.
30. H. Luo, C. Liu, D. He, J. Xu, J. Sun, J. Li and X. Pan, Environmental behaviors of microplastics in aquatic systems: A systematic review on degradation, adsorption, toxicity and biofilm under aging conditions, *Journal of Hazardous Materials*, 2022, **423**, 126915.
31. I. Nabi, K. Li, H. Cheng, T. Wang, Y. Liu, S. Ajmal, Y. Yang, Y. Feng and L. Zhang, Complete photocatalytic mineralization of microplastic on TiO2 nanoparticle film, *Iscience*, 2020, **23**, 101326.
32. L. Tian, Q. Chen, W. Jiang, L. Wang, H. Xie, N. Kalogerakis, Y. Ma and R. Ji, A carbon-14 radiotracer-based study on the phototransformation of polystyrene nanoplastics in water versus in air, *Environmental Science: Nano*, 2019, **6**, 2907-2917.
33. J. Duan, Y. Li, J. Gao, R. Cao, E. Shang and W. Zhang, ROS-mediated photoaging pathways of nano- and micro-plastic particles under UV irradiation, *Water Research*, 2022, **216**, 118320.
34. X. Li, S. Ji, E. He, W. J. G. M. Peijnenburg, X. Cao, L. Zhao, X. Xu, P. Zhang and H. Qiu, UV/ozone induced physicochemical transformations of polystyrene nanoparticles and their aggregation tendency and kinetics with natural organic matter in aqueous systems, *Journal of Hazardous Materials*, 2022, **433**, 128790.
35. Y. Liu, Y. Hu, C. Yang, C. Chen, W. Huang and Z. Dang, Aggregation kinetics of UV irradiated nanoplastics in aquatic environments, *Water Research*, 2019, **163**, 114870.
36. X. Wang, Y. Li, J. Zhao, X. Xia, X. Shi, J. Duan and W. Zhang, UV-induced aggregation of polystyrene nanoplastics: effects of radicals, surface functional groups and electrolyte, *Environmental Science: Nano*, 2020, **7**, 3914-3926.

37. A. Chamas, H. Moon, J. Zheng, Y. Qiu, T. Tabassum, J. H. Jang, M. Abu-Omar, S. L. Scott and S. Suh, Degradation Rates of Plastics in the Environment, *ACS Sustainable Chemistry & Engineering*, 2020, **8**, 3494-3511.
38. R. G. Kadhim, Study of some optical properties of polystyrene-Copper nanocomposite films, *World Scientific News*, 2016, **30**, 14.